Large-Signal Characterization of an 870MHz Inverse Class-F Cross-Coupled Push-Pull PA using Active Mixed-Mode Load-Pull

M. P. van der Heijden, D. M. H. Hartskeerl, I. Volokhine, V. Teppati*, and A. Ferrero*

Philips Research Laboratories, 5656 AE Eindhoven, The Netherlands, *Electronic Engineering Department, Politecnico di Torino, Torino, Italy (e-mail: m.p.van.der.heijden@philips.com)

***Abstract* — An inverse class-F cross-coupled push-pull PA in a 0.5um SiGe technology is presented. It is shown that inverse class-F in combination with C_{BC} compensation is preferred over class-F operation in terms of gain roll-off and efficiency as function of collector supply voltage. The active mixed-mode load-pull system is used to set up the proper output differential and common-mode impedances at the fundamental (870MHz) and harmonics to experimentally verify inverse class F operation with a measured PAE of 67% at 20dBm output power.**

***Index Terms* — active harmonic load pull, class F, inverse class-F, Mextram, power-added efficiency, push-pull power amplifier.**

I. Introduction

A clear trend is visible towards multi-mode mobile cellular applications that combine e.g. GSM, EDGE, and UMTS standards in a single transmitter. The conventional linear class-AB power amplifier (PA) is slowly abandoned to make place for superior solutions focusing on power efficiency, and thus longer battery life [1]. Polar systems, such as polar-loop transmitters, and true polar modulators are gaining more interest in the market [1]-[3]. In these architectures the envelope signal is impressed upon the RF carrier via the PA power supply. The PA in such systems is saturated or nearly saturated for high power efficiency depending on the TX architecture and standards involved.

This paper investigates class F and inverse class-F (IF) operation of a SiGe cross-coupled push-pull (CCPP) PA in QUBiC4G technology [4], [5]. Section III investigates the benefits of using a CCPP PA in a simulation experiment with MEXTRAM as the model for the devices [6]. To validate the conclusions from Section III, the simulated PA performance is experimentally verified in Section IV using the novel active harmonic mixed-mode load-pull setup [7].

II. Class-F and Inverse Class-F Operation

The analysis and implementation of high-efficiency modes of operation (e.g. class C, D, E, and F) has been subject of many studies and the basic operation is well understood [8]-[11]. A variety of modes of operation in-between classes C, E, and F are possible [8]. Class F increases efficiency and output power by using harmonic impedance control in the output matching to shape the collector (or drain) waveforms. In class F, the voltage waveform includes one or more odd harmonics and approximates a square wave, while the current includes even harmonics and approximates a half sine wave. Alternately, in class IF the voltage can approximate a half sine wave and the current a square wave. Class F and class IF operation are considered to be good candidates for our application and bandwidth requirements regarding efficiency and power output capability. The former depends only upon the number of harmonics and the latter depends upon the harmonic impedances as explained by Raab [8].

Other harmonic tuning strategies have been investigated in [10] and [11], where the focus is placed at both input and output harmonic tuning. Basically, the main efficiency enhancement mechanism in all of these tuning strategies is the collector voltage peaking using a high 2nd-harmonic output impedance. The analyses of these operating modes become very tedious as soon as more nonlinearities are taken into account. A good way to investigate class F and class IF is by using harmonic balance simulations (in ADS) with an accurate physics-based compact model of the bipolar device, such as MEXTRAM, as we see next.

III. Cross-Coupled Push-Pull PA

Fig. 1 shows a cross-coupled bipolar push-pull device, which has been fabricated for this experiment in a f_T = 50GHz 0.5µm high-voltage SiGe BiCMOS-process [5].

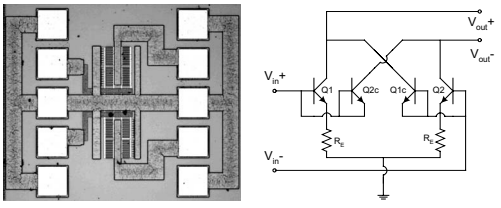

Fig. 1. Chip photograph of the fabricated cross-coupled push-pull device with an active emitter area of 640µm^2 and its simplified circuit schematic.

In this context cross-coupled means that bridge neutralization is used to compensate the parasitic negative feedback via the collector-base capacitance (C_{BC}) [4], [12]. This so-called C_{BC} compensation makes the amplifier unilateral, yielding high stable gain and high forward and reverse isolation. The high gain boosts the total PA power-added efficiency (PAE), since any driver stage preceding the amplifier will have minor influence on PAE. Especially in polar applications, the C_{BC} compensation also slightly decreases the gain roll-off as a function of collector voltage as we see later.

For the experiment, we optimized the fundamental, *second* harmonic common-mode (CM) and *third* harmonic differential-mode (DM) load impedances $Z_{Ln,C,D}$ (n is the harmonic number) of the 640μm^2 push-pull PA for class F and inverse class F. The DM and CM source terminations at the fundamental and harmonics are set to the characteristic impedance (100Ω DM and 25Ω CM). Table I summarizes the bias and all load impedance settings for this experiment. Note that in contrast with a single-ended design, the second and third harmonic in a differential amplifier are CM and DM signals, respectively.

TABLE I
BIAS AND LOAD SETTINGS FOR CLASS F AND CLASS IF

Class	$I_{C,Q}$ [mA]	$Z_{L1,D}$ [Ω]	$Z_{L2,C}$ [Ω]	$\Gamma_{L2,C}$	$Z_{L3,D}$ [Ω]	$\Gamma_{L3,D}$
F	18.5	95+45j	0.13-4j	0.99 ∠200°	4.3-275j	0.99 ∠-40°
F (no comp.)	14.5	100+35j	0.13-4j	0.99 ∠200°	4.3-275j	0.99 ∠-40°
IF	14.5	95+45j	∞	0.99 ∠0°	0.5-5j	0.99 ∠186°
IF (no comp.)	14.5	105+35j	∞	0.99 ∠0°	0.5-5j	0.99 ∠186°

The differential power gain and PAE at the fundamental can be calculated as

$$G_{pD} = P_{outD}/P_{inD}$$
$$PAE = \left(P_{outD} - P_{inD}\right)/P_{DC}, \quad (1)$$

where P_{inD} and P_{outD} are the differential-mode input power and output power and P_{DC} is the total DC power consumption of the CCPP PA.

Fig. 2 shows the simulated DM power gain and PAE as a function of DM output power at f_0 = 870 MHz with and without C_{BC} compensation. Clearly, inverse class-F and class IF have similar performance in terms of output power and efficiency but in class IF the maximum PAE occurs at a higher compressed output power as already shown by Inoue [9].

More interestingly is to see what happens if we vary the supply voltage V_{CC}. Fig. 3 shows the power gain and PAE versus differential output power. The supply voltage was swept according to the square law relation between signal power and supply voltage, assuming a constant gain:

$$P_{inD} \propto V_{CC}^2 \quad (2)$$

Fig. 3 shows that the combination of both C_{BC} compensation and inverse class F operation gives the best trade off between gain and efficiency as a function of V_{CC}, and consequently output power. The gain roll-off is slightly better (3dB) than without compensation (4dB). The efficiency improvement is significantly better (>10%.) than class-F at reduced supply voltage levels.

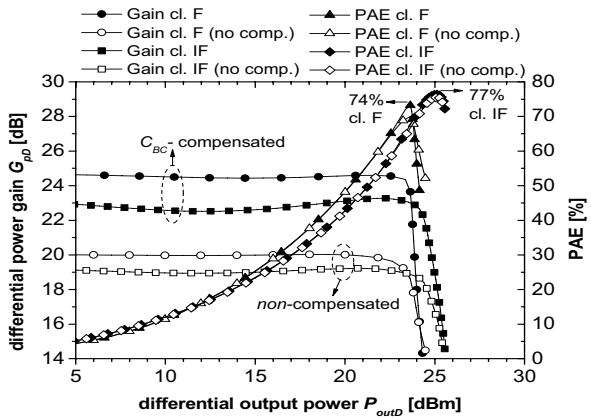

Fig. 2. Simulated class F and inverse class-F differential power gain and PAE versus differential output power for the 640μm^2 device at f_0 = 870 MHz biased at $I_{C,Q}$ = 14.5 mA for class F and 18.5 mA for class IF, and V_{CC} = 3.5 V.

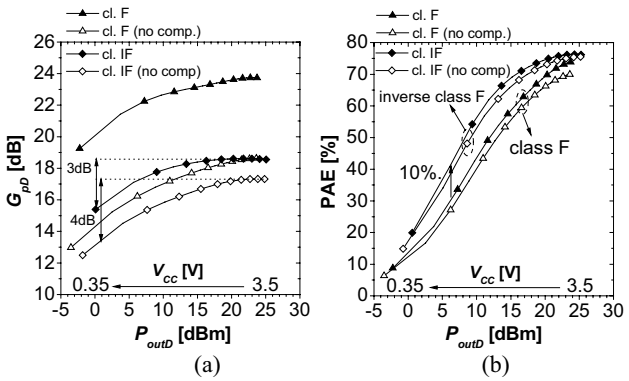

Fig. 3. Simulated class F and inverse class-F (a) differential power gain and (b) PAE versus differential output power with swept V_{CC} for the 640μm^2 device at f_0 = 870 MHz biased at $I_{C,Q}$ = 14.5 mA (class F) and 18.5 mA (class IF), and V_{CC} = 3.5 V.

The explanation for this can be found by examining the collector waveforms. It was found that in class F, the current waveform becomes more distorted when lowering V_{CC}, causing an increase of the amount of third harmonic

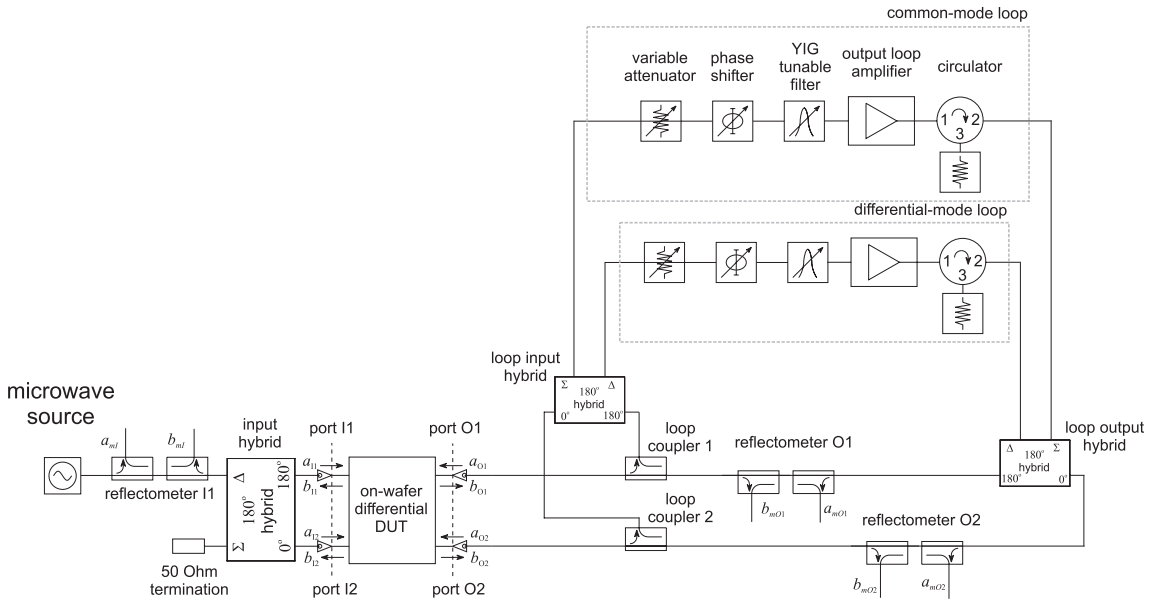

Fig. 4. Active differential/common-mode load used in the experiments.

content. This is similar to what Inoue [9] reported when increasing the load resistance in class F operation, since V_{CC} and R_L are inversely related for a certain P_{outD}. On the other hand, class IF also benefits from the high voltage swing and low current swing, which reduces the effect of the finite knee voltage of the device.

IV. Experimental Results

A. Active Mixed-Mode Load Pull System

Fig. 4 shows the differential/common-mode load-pull system, used to perform measurements. The basic principle of the active mixed-mode load is presented in [7]. The system is able to tune the device output differential and common-mode reflection coefficients, while the input differential reflection coefficient and power are being measured through a reflectometer I1. Note that the position of the loop couplers is as close as possible to the DUT, and the reflectometers inside the loop. This technique is crucial to avoid loop oscillation and it has been patented for a single ended active loop [13].

At the DUT output, this system measures differential and common-mode reflection coefficients and powers. These quantities are defined as

$$\Gamma_{outC,D} \equiv a_{outC,D} / b_{outC,D}$$
$$P_{outC,D} \equiv \left|b_{outC,D}\right|^2 - \left|a_{outC,D}\right|^2 = \left|b_{outC,D}\right|^2 \left(1 - \left|\Gamma_{outC,D}\right|^2\right), \quad (3)$$

where, according to Bockelman and Eisenstadt [14] notation

$$\begin{pmatrix} a_{outD} \\ a_{outC} \end{pmatrix} \equiv \frac{1}{\sqrt{2}} \begin{pmatrix} 1 & -1 \\ 1 & 1 \end{pmatrix} \begin{pmatrix} a_{O1} \\ a_{O2} \end{pmatrix} \quad (4)$$

$$\begin{pmatrix} b_{outD} \\ b_{outC} \end{pmatrix} \equiv \frac{1}{\sqrt{2}} \begin{pmatrix} 1 & -1 \\ 1 & 1 \end{pmatrix} \begin{pmatrix} b_{O1} \\ b_{O2} \end{pmatrix}. \quad (5)$$

The single-ended quantities a_{O1}, a_{O2} and b_{O1}, b_{O2} are measured in real-time, by reflectometers O1 and O2. The system is calibrated on-wafer with any classical load-pull calibration at ports O1 and O2 [15].

Once a_{O1}, a_{O2} and b_{O1}, b_{O2} are measured, all differential and common-mode quantities, for any required frequency, are easily carried out with equations (3)-(5). In this way, during the measurement, ports O1 and O2 act as a one-port mixed-mode reflectometer, which is connected to the differential/common-mode output of the device. Due to the lack of a complete 4-port system, this mixed-mode output reflectometer is coupled to a single port reflectometer I1 at the input.

It can be proved that, assuming an ideal input hybrid and with a particular calibration technique, reflectometer I1 is able to measure differential input power P_{inD} and gamma Γ_{inD}. In conclusion, the system is able to control and measure differential and common-mode, fundamental and harmonic output loads, to measure differential and common-mode, fundamental and harmonic output powers and to measure input differential power and gamma at the fundamental.

B. Measurement versus Simulation

The predicted MEXTRAM performance agrees very well with those measured as shown in Fig. 5 and 6, where we plotted the differential power gain and efficiency as a function of differential output power. In the load-pull experiments, we optimized the second harmonic load impedance ($Z_{L2,C}$) for inverse class-F operation. Due to some instability problems of the device we were limited in the choice of $Z_{L2,C}$ and not able to enforce class-F

operation. Instead we compare the results with $Z_{L2,C}$ = 16+3.8j Ω (low impedance) and denote this as 'conventional class-AB'.

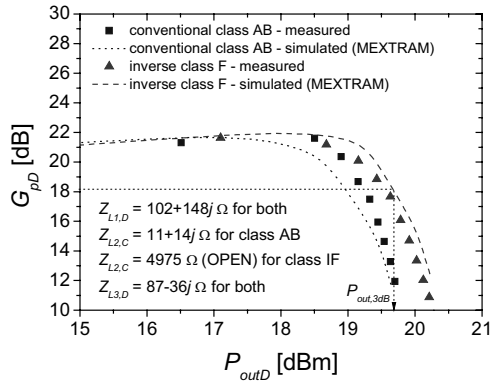

Fig. 5. Measured and simulated differential power gain versus differential output power for inverse class F and 'conventional class-AB' operation at f_0 =870 MHz, biased at $I_{C,Q}$ = 10 mA and V_{CC} = 3.0 V.

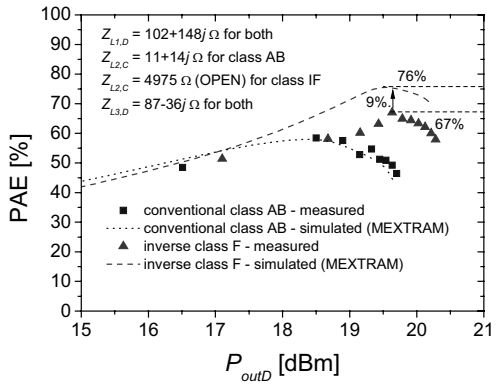

Fig. 6 .Measured and simulated power-added efficiency versus differential output power for inverse class F and 'conventional class-AB' operation at f_0 =870 MHz, biased at $I_{C,Q}$ = 10 mA and V_{CC} = 3.0 V.

The reduced PAE around 3 dB compression with respect to the simulations (9%.) can be explained by self-heating effects, which were not modeled for this device. The decrease in PAE has been verified in simulation by increasing the simulation temperature from 25° to 50°C.

V. Conclusion

This paper shows that a cross-coupled push-pull PA, working in inverse class-F mode offers advantages over a non-compensated or single-ended PA in terms of gain and power efficiency. Inverse class-F is the preferred operating class in terms of efficiency when supply voltage modulation is applied to the PA. A novel mixed-mode load-pull setup has been used to experimentally verify inverse class-F operation of a SiGe bipolar cross-coupled push-pull PA. This systems proves to be an excellent tool to investigate high-efficiency classes of operation in differential amplifier circuits.

Acknowledgement

The authors wish to acknowledge Dr. B. Minnis from the Wireless Group in Philips Research Redhill and the support of Atef Acknouck from Delft University of Technology.

References

[1] L. Larson, P. Asbeck, and D. Kimball, "Next Generation Power Amplifiers for Wireless Communications – Squeezing More Bits Out of Fewer Joules," *IEEE RFIC Symp. Dig*.,pp. 417-420, June 2005.

[2] T. Sowlati, et. al., "Polar loop transmitter for GSM / GPRS / EDGE," *IEEE RFIC Symp. Dig*., pp. 13-16, June 2005.

[3] G. Seegerer and G. Ulbricht, "EDGE Transmitter with Commercial GSM Power Amplifier Using Polar Modulation with Memory Predistortion," *IEEE MTT-S Digest*, pp. 1553-1556, June 2005.

[4] M.P. van der Heijden, M. Spirito, L.C.N. de Vreede, F. van Straten, and J. N. Burghartz, "A 2 GHz high-gain differential InGaP HBT driver amplifier matched for high IP3, " *IEEE MTT-S Digest*, vol. 1, pp. 235-238, June 2003.

[5] P. Deixler, et. al, "QUBiC4G: a f_T /f_{max} =70/100GHz 0.25µm low power SiGe-BiCMOS production technology with high quality passives for 12.5 Gb/s optical networking and emerging wireless applications up to 20 GHz," *Proceedings of the Bipolar/BiCMOS Circuits and Technology Meeting,* pp. 201-204, October 2002.

[6] http://www.semiconductors.philips.com/Philips_Models/bipolar/mextram/

[7] A. Ferrero and V. Teppati, "A novel active differential/common-mode load for true mixed-mode load-pull systems," *submitted for publication in IEEE Int. Microwave Symposium Digest*, June 2006.

[8] F. H. Raab, "Class-E, class-C, and class-F power amplifiers based upon a finite number of harmonics," *IEEE Trans. Microwave Theory Tech.*,vol. 47, pp. 1462–1468, Aug. 2001.

[9] A. Inoue, A. Ohta, S. Goto, T. Ishikawa, and Y. Matsuda, "The efficiency of class-F and inverse class-F amplifiers," *IEEE MTT-S Digest*, vol. 3, pp. 1947-1950, June 2004.

[10] F. van Rijs, et. al, "Influence of output impedance on power added efficiency of Si-bipolar power transistors," *IEEE MTT-S Digest*, vol. 3, pp. 1945-1948, June 2000.

[11] P. Colantonio, F. Giannini, G. Leuzzi, and E. Limiti, "Harmonic tuned PAs design criteria," *IEEE MTT-S Digest*, vol. 3, pp. 1639-1642, June 2002.

[12] J. A. Mataya, G. Haines, and S. B. Marshall, "IF amplifier using *Cc* compensated transistors," *IEEE J. Solid-State Circuits*, vol. 3, no. 4, pp. 401–407, Dec. 1968.

[13] A. Ferrero, *Active load or source impedance synthesis apparatus for measurement test set of microwave components and systems*, United States Patent no. 6509743, 12 June 2000.

[14] D. E. Bockelman and R. Eisenstadt, "Pure-mode network analyzer for on wafer measurements of mixed-mode S-parameters of differential circuits," *IEEE Trans. Microwave Theory & Tech.*, vol. 45, pp. 1071–1077, July 1997.

[15] A. Ferrero and U. Pisani, "An improved calibration technique for onwafer large-signal transistor characterization," *IEEE Trans. Instrum. Meas.*, vol. IM-47, pp. 360–364, April 1993.